PCM-TV-TFV: A Two Stage Framework for Image Reconstruction from Fourier Data

Weihong Guo

Case Western Reserve University, Cleveland, Ohio, USA

Joint work with
Yue Zhang, Siemens Corporate Research
Guohui Song, Clarkson University

BIRS, June 27th, 2019

Outline

1. Background
   - Image reconstruction
   - Continuous modeling methods
2. The proposed fidelity under PCM
   - Projection-Correction Modeling (PCM)
   - Optimal linear approximation
   - PCM with TV
3. The proposed regularity
   - Fractional order variational methods
   - TV-TFV: global and local
4. A combined model
5. Conclusions

Outline

Image reconstruction

- Problem: Recover signals or images from its samples in a sampling domain. Mathematically, retrieve f from

$$\hat{f} = S\mathcal{F}f + \epsilon,$$

  S: Sampling operator, $\mathcal{F}$: Fourier transform, Radon transform etc. ϵ: noise.
- Challenges:
  - Appearance of noise
  - Non-uniformess of measurements
  - ...
- Application: radar imaging, medical imaging (MRI), electron microscopy etc.

Continuous modeling Methods

- General idea:
  1. Suppose $f \approx \sum_{i=1}^{n} c_i \phi_i := \Phi c$ with $c \in \mathbb{R}^n$, where $\phi_i's$ form the continuous basis of the space $\mathcal{H}_n = span\{\phi_i, 1 \leq i \leq n\}$, we call $\mathcal{H}_n$ as *the processing space*.
  2. Solve c with given samples $\hat{f}$ from

$$\hat{f} = S\mathcal{F}f + \epsilon = S\mathcal{F}\Phi c + \epsilon := \mathcal{T}c + \epsilon \Rightarrow \frac{1}{2}\|\hat{f} - \mathcal{T}c\|^2 + \mathcal{R}(c)$$

  3. Reconstruct $\bar{f} = \Phi c$.
- Methods:
  - Generalized sampling [Adcock, Hansen, 2015]
  - RKHS methods [Deng, G. and Huang, 2015]
  - Frame-based methods [Gelb, Song, 2014, Alberti, Santacesaria 2019]
  - ...

Outline

Projection-Correction Modeling (PCM)

A general **PCM** with Fourier measurements:

1. First stage (projection): solve $\hat{c}$ from

$$\hat{c} = \underset{c}{\operatorname{argmin}} \|\mathcal{T}c - \hat{f}\|_2^2$$

where $\mathcal{T}_{kj} := (\mathcal{F}\Phi)_{kj} = \langle e_k, \phi_j \rangle$, $e_k = e^{-2\pi i w_k t}$, ϕ_j is the jth basis vector of the processing space $\mathcal{H}_n$.

2. Second stage (correction): solve c from

$$c = \underset{c}{\operatorname{argmin}} \frac{1}{2}\|c - \hat{c}\|_2^2 + \lambda \mathcal{R}(c)$$

where $\mathcal{R}(c)$ can be $\|c\|_1$, $\|\nabla \Phi c\|_1$, $\|\nabla \Phi c\|_2^2$, $\|\Psi(\Phi c)\|_1$ etc.

One Vs. Two

- Proposed

$$\min_c \frac{1}{2}\|c - (\mathcal{F}\Phi)^\dagger \hat{f}\|_2^2 + \lambda \mathcal{R}(c)$$
$$\Rightarrow c - (\mathcal{F}\Phi)^\dagger \hat{f} + \lambda \partial \mathcal{R}(c) = 0$$

- Single fidelity

$$\begin{aligned} & \min_c \frac{1}{2}\|(\mathcal{F}\Phi)c - \hat{f}\|_2^2 + \lambda \mathcal{R}(c) \\ \Rightarrow \quad & (\mathcal{F}\Phi)^*(\mathcal{F}\Phi)c - (\mathcal{F}\Phi)^* \hat{f} + \lambda \partial \mathcal{R}(c) = 0 \\ \Rightarrow \quad & c - (\mathcal{F}\Phi)^\dagger \hat{f} + \lambda((\mathcal{F}\Phi)^*(\mathcal{F}\Phi))^{-1} \partial \mathcal{R}(c) = 0 \end{aligned}$$

Optimal linear approximation

- **Fourier frames** [Song, Gelb 2013]: If the processing basis $\{\phi_i\}_{i=1}^n$ is *intrinsically localized* w.r.t. sampling scheme $\{e_k\}_{k=1}^m$,

$$|\langle e_j, \phi_l \rangle| \le c_0(1 + |j - l|)^{-s}, \text{ for } c_0 > 0, s > \frac{1}{2}, j, l \in \mathbb{N}$$

  then $\|\mathcal{P}_{H_n} f - f\|_2 \le cn^{-(t-1/2)}$ where $t \ge s$ depends on ϕ.
- **Wavelets**: For a wavelet ψ with q vanishing moments, given a function $f \in L^2[0,1]$ in $W^s[0,1]$, the approximation by first $N = 2^R$ wavelet basis generated by ψ achieves the decay error $o(N^{-2s})$ with $q > s$.

PCM with Total Variation

The PCM-TV model:

$$\mathbf{P}: \min_{cf} \|\mathcal{T}c_f - \hat{f}\|_2^2, \qquad \mathbf{C}: \min_{c_g} \frac{1}{2}\|c_g - c_f\|^2 + \lambda \|\nabla(\Phi c_g)\|_1$$

A general two-stage PCM-TV algorithm:

1. Choose proper basis Φ, compute transition operator $\mathcal{T}$.
2. Projection: solve for $c_f = \mathrm{argmin}_{c_f} \|\mathcal{T}c_f - \hat{f}\|_2^2$.
3. Correction: initialize $c_g^1 = c_f$. For $k = 1, 2, ...$, iterate update

$$\begin{aligned} c_g^{k+1} &= \operatorname*{argmin}_{c_g} \frac{1}{2}\|c_g - c_f\|^2 + \lambda \|\nabla \Phi c_g - d^k + b^k\|_2^2, \\ d^{k+1} &= shrink(\nabla \Phi c_g^{k+1} + b^k, 1/\lambda), \\ b^{k+1} &= b^k + \gamma(\nabla \Phi c_g^{k+1} - d^{k+1}), \end{aligned}$$

until convergence.

Comparison between different models

Recall $\mathcal{R}(c)$ stands for the choice of regularity in the correction step. Here we compare different models for reconstruction from Fourier measurements:

- Proposed PCM-TV with $\mathcal{R}(c) = \|\nabla\Phi c\|_1$.
- Generalized Sampling with $\mathcal{R}(c) = \|c\|_1$.
- Tikhonov with $\mathcal{R}(c) = \|c\|_2^2$.
- Single stage TV,

$$\min_c \frac{1}{2}\|\mathcal{T}c - \hat{f}\|_2^2 + \lambda\|\nabla\Phi c\|_1.$$

Numerical Experiments

Two different bias cases:

- Reconstruction with Bias-free, i.e. $f \in \mathcal{H}_n$.
- Reconstruction with Bias error, i.e. $f \notin \mathcal{H}_n$, however $\|\mathcal{P}_{\mathcal{H}_n} f - f\|_2 \to 0$, as $n \to \infty$.

Different distributions of $\hat{f} \in \mathbb{C}^m$:

- Uniform distributed sampling, $w_k = k$, $k = -m/2, -m/2+1, ..., m/2-1$.
- Jittered sampling, $w_k = k + \eta_k$, $\eta_k \sim U[-\theta, \theta]$.

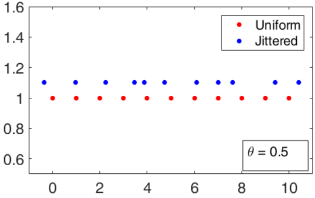

In the experiments, $\mathcal{H}_n$ is spanned by Haar wavelet.

Numerical Experiments in 1D

Bias free from nonuniform Fourier measurements without noise:

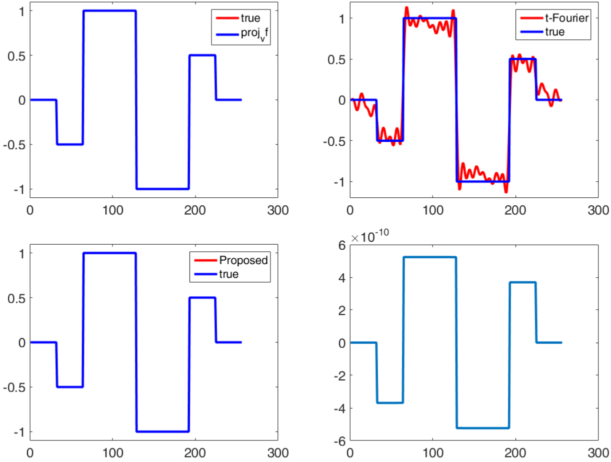

Figure: $m = 128$, $n = 32$, $resol = 1/256$, $\theta = 0.25$.

Reconstruction with bias error, $n = 128$:

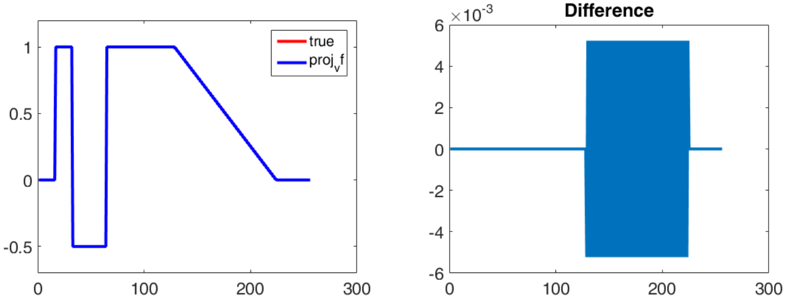

Reconstruction with bias error, $n = 128$:

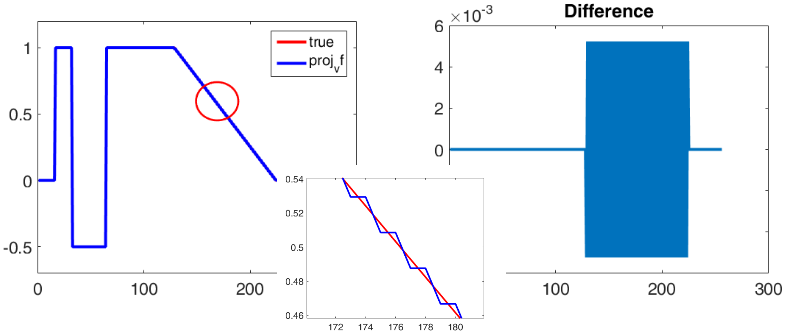

Reconstruction with bias and noise ϵ:

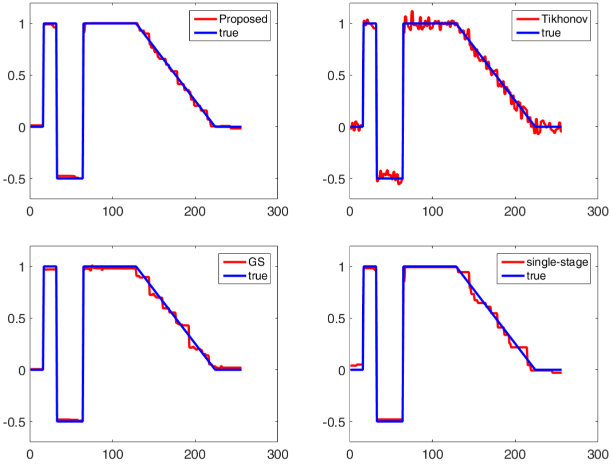

Figure: $m = 256$, $n = 128$, level of noise $\sigma := \|\epsilon\|_2 / \|\hat{f}\|_\infty = 0.2$, $\theta = 0.5$.

Quantitative Performance Comparison (different σ)

Fix $m = 256$, $n = 128$, $\theta = 1/4$, we have

σ	Model	ssim	psnr	snr	rela_err
0.1	Proposed	**0.9283**	**39.14**	**33.58**	**0.0161**
	GS	0.8478	36.45	30.88	0.0220
	SS-TV	0.8466	35.72	30.16	0.0239
	Tikhonov	0.7640	32.17	26.60	0.0360
0.4	Proposed	**0.8505**	**29.41**	**23.84**	**0.0495**
	GS	0.7092	26.21	20.64	0.0715
	SS-TV	0.6830	23.81	18.24	0.0942
	Tikhonov	0.3041	21.09	15.52	0.1289
0.7	Proposed	**0.7096**	**24.87**	**19.30**	**0.0834**
	GS	0.6221	21.93	16.36	0.1170
	SS-TV	0.6816	22.60	17.03	0.1083
	Tikhonov	0.1414	15.51	9.951	0.2445

Quantitative Performance Comparison (different n)

Fix $\sigma = 0.2$, $m = 256$, $\theta = 1/4$, we have

n	Model	ssim	psnr	snr	rela_err
32	Proposed	**0.8758**	32.98	27.41	0.0328
	GS	0.8475	**33.30**	**27.73**	**0.0316**
64	Proposed	**0.8755**	**33.40**	**27.83**	**0.0313**
	GS	0.8046	32.54	26.97	0.0345
96	Proposed	**0.8494**	**33.76**	**28.19**	**0.0300**
	GS	0.7941	32.30	26.73	0.0355
128	Proposed	**0.8698**	**34.20**	**28.63**	**0.0285**
	GS	0.7917	32.06	26.49	0.0365

Model Comparisons in 2D

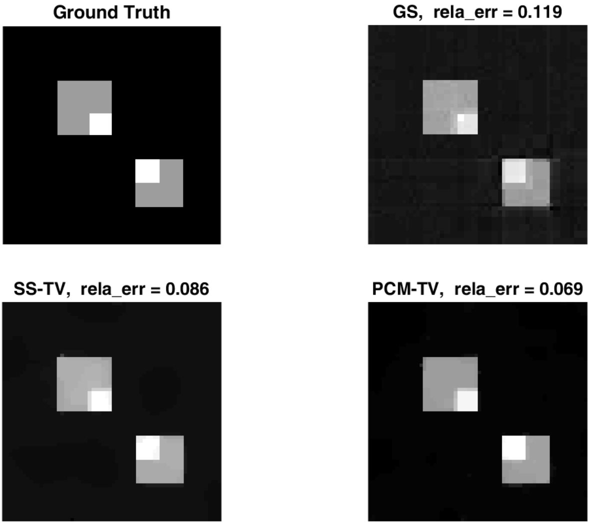

Figure: $m = 128 \times 128$, $n = 64 \times 64$, $imsize = 256 \times 256$, $\sigma = 0.6$.

Model Comparisons in 2D

Numerical details,

Model	psnr	snr	rela_err
GS	30.9673	18.0176	0.1188
SS-TV	33.8196	20.87	0.086
PCM-TV	**35.6589**	**22.7092**	**0.069**

Outline

Fractional order variational methods

It has been shown that the fractional order variational methods performs as a well trade-off between *TV* and *Laplacian* methods.

- [Bai, Feng 2007] first introduced the anisotropic diffusion equations for image reconstruction

$$\frac{\partial u}{\partial t} = -D_x^\alpha * (c(|D^\alpha u|)D^\alpha u) - D_y^\alpha * (c(|D^\alpha u|)D^\alpha u)$$

- [Chen et al. 2013] showed the advantages of total fractional order variational model

$$\min_u \{E(u) := \int_\Omega \sqrt{(D_x^\alpha u)^2 + (D_y^\alpha u)^2} d\Omega + \frac{\lambda}{2}\|u - f\|_2^2\}$$

- [Zhang and Chen 2015] showed the TFV has a very comparable performance with TGV and mean curvature methods.

Fractional differential

- Different definitions: Riemann-Liouville (R-L), Grunwald-Letnikov and Caputo $\alpha-$order derivative etc.
- R-L $\alpha-$order derivative of $f(x)$ on $[a, b]$:

$$D^{\alpha}_{[a,x]} f(x) = \frac{1}{\Gamma(n-\alpha)} (\frac{d}{dx})^n \int_a^x \frac{f(\tau)}{(x-\tau)^{\alpha-n+1}}$$

$$D^{\alpha}_{[x,b]} f(x) = \frac{(-1)^n}{\Gamma(n-\alpha)} (\frac{d}{dx})^n \int_a^x \frac{f(\tau)}{(\tau-x)^{\alpha-n+1}}$$

$$D^{\alpha}_{[a,b]} f(x) = \frac{1}{2} (D^{\alpha}_{[a,x]} f(x) + (-1)^n D^{\alpha}_{[x,b]} f(x))$$

Where $0 \leq n-1 < \alpha < n$, $n \in \mathbb{Z}_+$.

Discretization of Fractional Derivative

The fractional-order differential is a global operator. This becomes more clear in its discretized form:

$$D_x^\alpha = \begin{pmatrix} 2w_1^\alpha & w & w_3^\alpha & \dots & w_N^\alpha \\ w & 2w_1^\alpha & \ddots & \ddots & \vdots \\ w_3^\alpha & \ddots & \ddots & \ddots & w_3^\alpha \\ \vdots & \ddots & \ddots & 2w_1^\alpha & w \\ w_N^\alpha & \dots & w_3^\alpha & w & 2w_1^\alpha \end{pmatrix},$$

where $w = w_0^\alpha + w_2^\alpha$, $w_0^\alpha = 1$, $w_j^\alpha = (1 - \frac{1+\alpha}{j})w_{j-1}^\alpha$, for $j = 1, ..., N+1$.

TV-TFV model

We propose a reconstruction model with a new regularity fusing the TV and TFV, which is

$$\min_{f} \frac{1}{2}\|f - \hat{f}\|^2 + \mu_t \|\nabla f|_{\Gamma}\|_1 + \mu_f \|\nabla^{\alpha} f|_{\Gamma^c}\|_1,$$

where Γ i s an open domain centered around the 'edge' set. This part is done similarly to the previous work [G., Yin 2012].

TV-TFV, details

- Warm up and select the edge $\bar{\Gamma}$.
  1. ROF for a few steps, in our experiment $3 \sim 5$, depends on the rough estimation of the noise level.
  2. Use edge filer such as ‘canny’ to get the edge set, this can be done quite efficiently.
- Image binary morphology: dilation operation to get Γ.

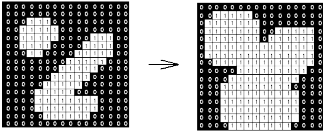

- Thresholding. Suppose during the iterations we get $\bar{\Gamma}_1$, $\bar{\Gamma}_2$,...$\bar{\Gamma}_n$, which acts as an time sequence. We will correct $\bar{\Gamma}_n$ with point-wise confidence level t.

TV-TFV Algorithm Framework

1. Initialize $\bar{\Gamma}_0 = \Omega$, $f^1 = \hat{f}$, decide confidence level t, length of stored sequence n.
2. Warm up with $3 \sim 5$ TV iterations and update $\bar{\Gamma}_0$ to $\bar{\Gamma}_1$.
3. For $k = 1, 2, ...,$
   - if $k > n$, $\bar{\Gamma}_k = (\sum_{i=k-n+1}^{k} \bar{\Gamma}_i) > n * t$; end
   - update $\Gamma_k = \text{dilate}(\bar{\Gamma}_k)$;
   - update $d^k = \nabla f|_{\Gamma_k}$, $e^k = \nabla^\alpha f|_{\Gamma_k^c}$.
   - Solve f-subproblem

$$f^{k+1} = \underset{f}{\text{argmin}} \frac{1}{2}\|f - \hat{f}\|_2^2 + \mu_t \|\nabla f|_{\Gamma_k} - d^k + dd^k\|_2^2 + \mu_f \|\nabla^\alpha f|_{\Gamma_k} - e^k + ee^k\|_2^2$$

   d-subproblem $d^{k+1} = shrink(\nabla f^{k+1}|_{\Gamma_k} + dd^k, \mu_t/\lambda_t)$
   dd-subproblem $dd^{k+1} = dd^k + \gamma_1(\nabla f^{k+1}|_{\Gamma_k} - d^{k+1})$
   similarly operations on $e-$ and $ee-$subproblem.

until convergence.

TV-TFV on Pure Denoising Problem

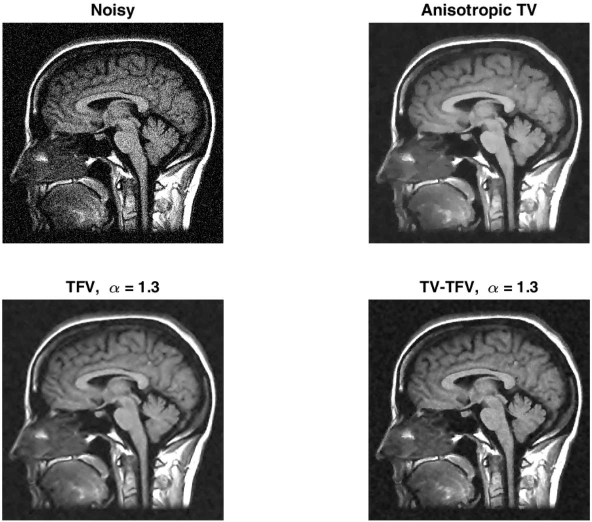

Image retrieved from `http://radiopaedia.org/` *by Frank Gaillard.*

TV-TFV on Pure Denoising Problem

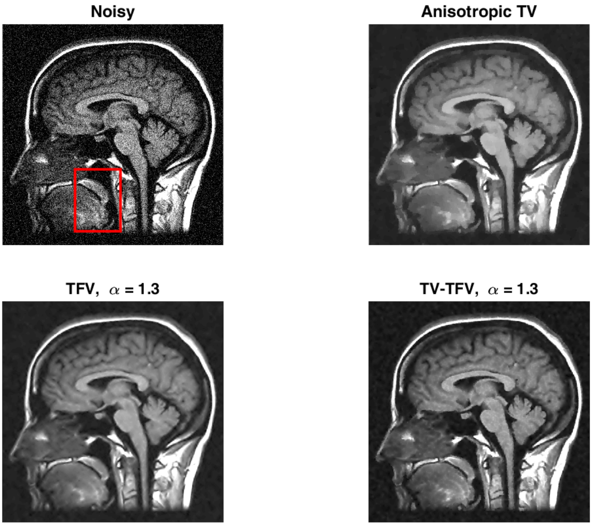

Image retrieved from `http://radiopaedia.org/` *by Frank Gaillard.*

TV-TFV on Pure Denoising Problem

Edge details,

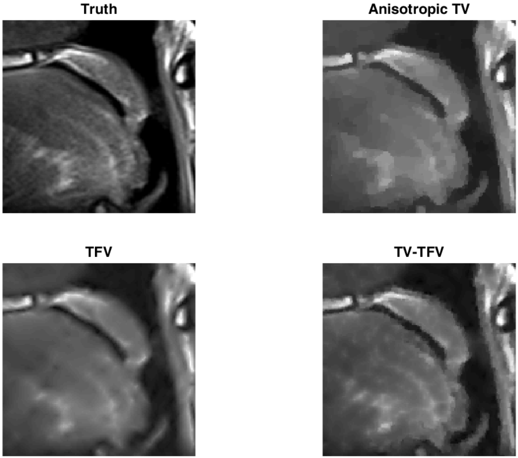

Figure: SSIM detail: TV: 0.6779, TFV: 0.6943, TV-TFV: 0.7281.

TV-TFV on Pure Denoising Problem

Numerical details,

Model	psnr	snr	rela_err
Noisy	20.9199	6.0853	0.3914
TV	31.0007	16.1661	0.1226
TFV	31.6910	16.8565	0.1133
TV-TFV	**32.1948**	**17.3602**	**0.1069**

Outline

All together: PCM with TV-TFV

We propose the combined reconstruction model:

$$\mathbf{P}: \quad c_f = \underset{c}{\operatorname{argmin}} \|\mathcal{F}(\Phi c) - \hat{f}\|_2^2$$

$$\mathbf{C}: \quad \min_{c_g} \frac{1}{2}\|c_g - c_f\|^2 + \mu_t \|\nabla g|_\Gamma\|_1 + \mu_f \|\nabla^\alpha g|_{\Gamma^c}\|_1$$

$$s.t. \quad g = \Phi c_g.$$

The algorithm will be a combination of the previous two.

PCM with TV-TFV

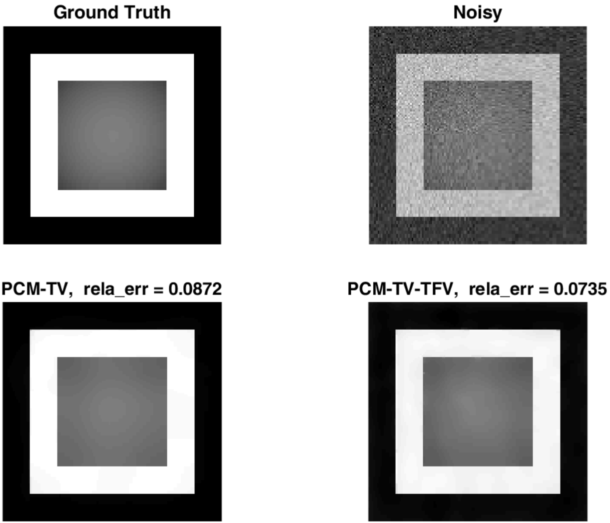

Figure: $m = 128 \times 128$, $n = 96 \times 96$, $imsize = 256 \times 256$, $\sigma = 0.4$.

PCM with TV-TFV

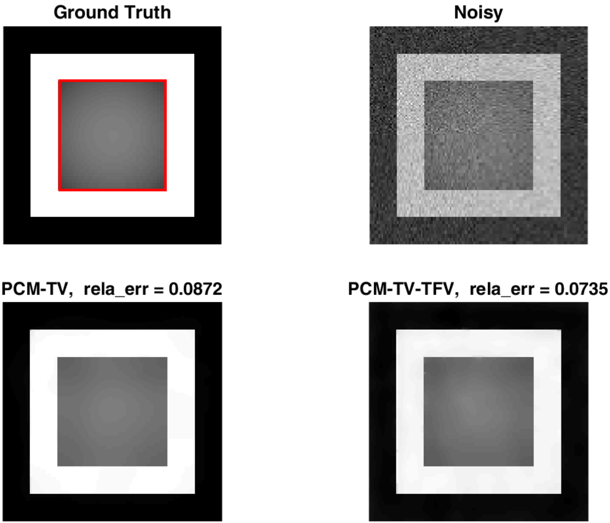

Figure: $m = 128 \times 128$, $n = 96 \times 96$, $imsize = 256 \times 256$, $\sigma = 0.4$.

PCM with TV-TFV

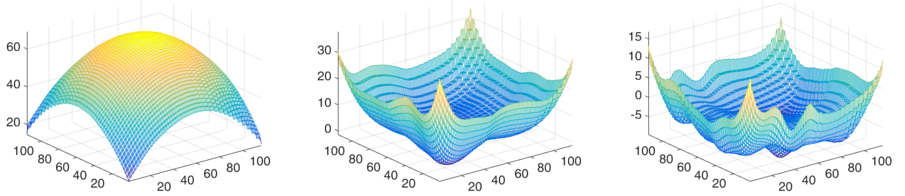

(a) Groud Truth (b) PCM-TV, err ≈ 62% (c) PCM-TV-TFV,err ≈ 32%

Figure: Fig (a) is the true surface, Figure (b) and (c) shows the differences between the truth and the reconstructed surface.

Outline

Conclusions

- We proposed a fidelity in a processing space instead of the classical sampling domain, under PCM framework.
- The new edge-based regularity TV-TFV shows the better performance than single TV or TFV models.
- A concrete PCM-TV-TFV model is built to combine the advantages of the two and further improve the performance.

Acknowledgment

This project is partially supported by NSF.

Discussion with Yiqiu Dong.

References

A. Gelb, and G. Song, A frame theoretic approach to the nonuniform fast fourier transform,

SIAM J. Numerical Analysis, 2014.

B. Adcock, and A. Hansen, Generalized sampling and infinite dimensional compressed sensing, Found. Comput. Math, 2015.

L. Deng, W. Guo, and G. Song, Single image super-resolution via an iterative reproducing kernel Hilbert space method, 2015.

W. Guo, and W. Yin, Edge guided reconstruction for compressive imaging, SIAM Journal on Imaging Sciences, 2012.

J. Zhang, and K. Chen, A total fractional-order variation model for image restoration with nonhomogeneous boundary conditions and its numerical solution, SIAM Journal on Imaging Sciences, 2015.

D. Chen, S. Sun, C. Zhang, Y. Chen, D. Xue, Fractional-order TV-l2 model for image denoising, Central European Journal of Physics, 2013.

Guo,W., Song,G. and Zhang,Y., PCM-TV-TFV: A novel two stage framework for image reconstruction from Fourier data, SIAM Journal on Imaging Sciences, 2017.

Thank you!